We are IntechOpen,
the world's leading publisher of
Open Access books
Built by scientists, for scientists

6,900
Open access books available

185,000
International authors and editors

200M
Downloads

154
Countries delivered to

Our authors are among the

TOP 1%
most cited scientists

12.2%
Contributors from top 500 universities

CLARIVATE ANALYTICS
BOOK CITATION INDEX
INDEXED

WEB OF SCIENCE™

Selection of our books indexed in the Book Citation Index
in Web of Science™ Core Collection (BKCI)

Interested in publishing with us?
Contact book.department@intechopen.com

Numbers displayed above are based on latest data collected.
For more information visit www.intechopen.com

Sound Absorbing Resonator Based on the Framed Nanofibrous Membrane

Klara Kalinova

Abstract

The sound absorbing means are based on a resonance membrane formed by a layer of polymeric nanofibers, which is restricted by a frame. The resonance membrane is then, upon impact of sound waves, brought into forced vibrations, whereby the kinetic energy of the membrane is converted into thermal energy by friction of individual nanofibers, by the friction of the membrane with ambient air and possibly with other layers of material arranged in its proximity. Moreover, part of the kinetic energy of the membrane is transmitted to the frame, to which the membrane is securely attached, and other part is converted into thermal energy due to increased friction in its inner structure, which is caused by the fact that the neighboring parts of the membrane, separated at least partially by the frame or its elements, may vibrate with mutually different periods and/or deviations. The frame is formed by a mesh of grid that can be regular in order to obtain uniform properties over the whole area of the sound absorbing material. The size and shape of the mesh affect the sound absorption or more precisely resonance behavior of the means. To obtain desired sound absorbing characteristics, the resonance membrane is connected to the frame with positive, zero, or negative tension.

Keywords: nanofibers, membrane, resonator, sound absorption, frame

1. Introduction

1.1 Membrane for sound absorption

The term oscillating membrane means a thin plate or foil which has a very small bending stiffness and is located at a distance from the fixed wall. The behavior of such a membrane can be compared to the behavior of a body of a certain weight (represented by a membrane) elastically attached to the spring (represented by an air cushion). The space between the membrane and the rear fixed wall is filled with a porous material that dampens the vibrations of air particles in this space and thus the whole system. Typically, the membrane is selected from such a fabric that its flexural stiffness is much smaller than that of an air cushion [1].

Membrane absorbers are used to absorb low frequency sound. In order to increase the sound absorption, the membrane is positioned at a certain distance parallel to the rigid wall, thus creating an air gap between the wall and the membrane. Coates and Kierzkowski [2] in their paper describe the advantages of thin,

light membranes that can replace traditional bulky and economically disadvantageous porous absorbers. The work deals with individual parameters such as the size of the air gap; membrane absorber thickness; its density, flexibility, and, in particular, air flow resistance; and its influence on sound absorption coefficient. The study [3] examines in detail the properties of a simple permeable membrane. The effect of membrane parameters such as basis weight and air flow resistance is clarified. The study is based on the theoretical solution presented in [4] for the perpendicular impact of sound waves. The permeable membrane is characterized by basis weight, tension, and air flow resistance R_h, which is a function of the thickness of the membrane. The influence of air flow resistance R_h to the sound absorption coefficient α occurs especially at higher frequencies. For extreme values, sound absorption coefficient α is zero. This is the case with extremely low air flow resistance R_h when all sound energy passes through the membrane. In the case of a very high R_h value, the membrane becomes impermeable, and all the sound energy is reflected. The optimal R_h value varies with the sound frequency and basis weight of the membrane. The influence of the basis weight is evident especially at lower frequencies. For higher sound frequencies, the value of α is almost constant. Thus, the basis weight loses the effect at higher frequencies, and only R_h plays the dominant role.

In the study [5, 6], the complete form of the analytical solution of the membrane sound absorption coefficient was described. A membrane of infinite dimensions lying in a plane parallel to the fixed wall at a certain distance is envisaged. The membrane characterized by the basis weight and the tension is vibrating by the impact of the plane wave below a given angle of incidence. Both side surfaces of the membrane, the source and back sides, as well as the wall surface, are described by a specific acoustic admittance. The sound absorption coefficient expresses the amount of energy absorbed, including energy losses of different types, which may be caused by different mechanisms at different locations in the system. The frequency of the α maxima, which is caused by the resonance of the system, decreases with the growth of the basis weight. The highest peak of α is recorded in a sample basis weight of $2\,\text{kg}\,\text{m}^{-2}$. With the increasing acoustic admittance of the back side of the membrane, sound absorption coefficient increases in frequency range up to 2 kHz; above this frequency, no effect of surface admittance on the back side, α is constant. Therefore, it can be argued that the sound absorption at higher frequencies is affected mainly by the acoustic admittance of the surface of the source side of the membrane.

A double resonant element, an acoustic element composed of two membranes separated by an air gap, was investigated in studies [7, 8]. Four types of two-layered resonant elements were measured, differing in basis weights [7]. The first membrane positioned in the direction of the incident sound wave always had a substantially smaller (approx. 10x) basis weight over the second membrane. The experimental results were in good agreement with the theoretical model. Furthermore, the influence of the thickness of the air gap, the weight of the two membranes, and their air flow resistance R_h were investigated. The study [8] also monitors the effect of airflow resistance of the first membrane on the acoustic behavior system. In this case, however, the first membrane positioned in the direction of the incident sound waves was permeable, characterized by an air flow resistance R_h.

The permeability of the membrane with optimal air flow resistance improves the absorption properties in the high sound frequency band. At low frequencies, the sound absorption coefficient increases with increasing mass of the first permeable membrane, while it decreases with increasing mass of the second solid membrane. Any effect of membrane mass on sound absorption coefficient is not found at

frequencies higher than 2 kHz. At low frequencies the characteristics are independent on air cavity between both membranes. At high frequencies, they are similar to those of a permeable membrane with an air back cavity and a rigid back wall.

The mechanical analogy can be compared to linear electric circuit theory [9]. The electric impedance is defined by the ratio of voltage and current. The acoustic impedance is established analogous to electric impedance as a ratio of sound pressure and acoustic volume velocity. In order to obtain the acoustic impedance of the whole system, the acoustic impedance of the individual elements was first calculated. The relationship was then obtained for calculating the sound absorption coefficient. Two types of glass fiber fabric and a microperforated synthetic membrane were measured to confirm this theory. Measurements took place in both the reverberation room and the impedance tube. The results obtained theoretically are in good agreement with the measured values. A honeycomb structure, or a hexagonal structure, can create a lightweight and stable frame of the acoustic membrane element. Such an absorber studied at work [10] is designed for room acoustics as well as for industrial applications.

In many other studies, various modifications of the oscillating membrane clamped in a circular frame are discussed. Determining the exact solution of oscillations of the circular membrane with inhomogeneous density was studied in works [11–15]. The study [16] focuses on the research of the base frequency of the circular membrane with additional star-shaped distortion originating from the outer edge. It is clear from the results that the base frequency increases with an increasing number of evenly distributed breaches and a length of breach. The article [17] describes the results of the research of the base frequency of a circular membrane that is in contact with water. It is known that the base frequencies of the structures in the water are smaller than in the air, due to the increase in the total kinetic energy of the system due to the presence of water.

1.2 Resonance frequency of membrane

1.2.1 Resonance frequency of circular membrane

A thin circular membrane is a formation that results, for example, from the tension of a thin homogeneous elastic film with a constant basis weight of m_{sq} (kg m^{-2}) on a rigid circular frame [18]. By this tension caused by the radially acting force F_r, the membrane gains its stiffness. The radially acting tensile force relative to the unit length of the frame circumference is constant in all directions, and then the tension ν (N m^{-1}) is given by the formula:

$$\nu = \frac{F_r}{2\pi R},$$ (1)

where F_r (N) is the total tensioning force and R (m) denotes the radius of the membrane (or the radius of the rigid circular support through which the membrane is tensioned). We expect this tension acting in the plane of the membrane to be the same in all places. Apart from circular membranes, other membrane shapes are used in applications, e.g., elliptical, rectangular membranes.

If the membrane deflects from a normal position (e.g., by acoustic pressure), the membrane that originally formed the plane surface is deformed. If the force that causes the deflection ceases to occur, all the membrane points return; their potential energy, which they get by the deflection, changes into kinetic energy of the moving substantial elements, and the membrane vibrates. If the damping is not taken into account, the membrane will vibrate with free undisturbed vibrations.

If the assumption of axially symmetrical vibrations is fulfilled, then the following relation (2) applies, from which it is possible to determine the base membrane frequencies $f_{0,i}$ (Hz) using the constant of the vid $a_{0,i}$ (equal to 2.4048 for $f_{0,1}$, 5.5201 for $f_{0,2}$, 8.6537 for $f_{0,3}$, 11.97915 for $f_{0,4}$):

$$f_{0,i} = \frac{1}{2\pi R} a_{0,i} C_M, \tag{2}$$

where C_M (m s^{-1}) is the velocity of transverse wave propagating on the membrane given by the relationship

$$C_M = \sqrt{\frac{\nu}{m_{sq}}}, \tag{3}$$

where m_{sq} (kg m^{-2}) is the basis weight of the membrane.

To calculate the membrane base frequencies according to formula Eq. (2), it is necessary first to determine the velocity of the transverse wave propagating on the membrane C_M. This is not possible without knowledge of the radially acting tensioning force v that causes the diaphragm tension on the circular frame. The C_M and ν values are not known, so Eq. (2) cannot be applied to the calculation. By adjusting it, however, the necessary relationships can be obtained.

For determining the angular velocity $\omega_{0,i}$ (s^{-1}), the following formula is commonly used:

$$\omega_{0,i} = 2\pi f_{0,i}. \tag{4}$$

By putting it in relation Eq. (2), the equation Eq. (4) can be rewritten as follows:

$$2\pi f_{0,i} = \frac{a_{0,i} C_M}{R}. \tag{5}$$

After the conversion of this relationship, it is possible to express the relation

$$f_{0,i} = \frac{a_{0,i} C_M}{2\pi R} \Rightarrow \frac{f_{0,i}}{a_{0,i}} = \frac{C_M}{2\pi R}. \tag{6}$$

The ratio $\frac{C_M}{2\pi R}$ is constant since the membrane radius and the velocity of the wave propagation by the membrane do not change. Thus, the ratio of frequency and relevant constant of the vid is constant as follows:

$$\frac{f_{0,1}}{a_{0,1}} = \frac{f_{0,2}}{a_{0,2}} = \frac{f_{0,3}}{a_{0,3}} = \frac{f_{0,4}}{a_{0,4}}. \tag{7}$$

From the abovementioned relationships Eqs. (4)–(6), it is obvious that the radius of the membrane R is inversely proportional to the frequency $f_{0,i}$ and with the increasing radius of the membrane, the own frequency falls.

1.2.2 Resonance frequency of rectangular membrane

The membrane is tensioned in the *x-axis* and *y-axis* direction by a tension ν applied per unit length. The rectangular membrane with sides a and b and axes x and y is tensioned in axial direction by forces:

$$F_x = b.\nu, F_y = a.\nu \tag{8}$$

For the rectangular membrane, its resonant frequency $f_{m,n}$ (Hz) according to the work [18] is given by the relation

$$f_{m,n} = \frac{1}{2}C_M \sqrt{\left(\frac{m}{a}\right)^2 + \left(\frac{n}{b}\right)^2},$$ (9)

where m and n are vids in each axis and a and b (m) are the dimensions of the sides of the rectangle.

The nodal lines of the circle in the simplest case of symmetry are concentric circles, the node lines of the rectangle pointing in the simplest case in the direction of the membrane stresses (perpendicular to the sides of the shape) and dividing the rectangle into the same parts in either direction or in both directions. In a more complex case, the node line is guided along the diagonal rectangle. The constant tension of the membrane ν was achieved by observing the constant conditions during the electrospinning of nanofibrous membrane to the grid support. The optical method according to study [19] determined the base resonant frequency of the circular membrane $f_{0,i}$. Assuming a constant value ν and thus C_M, then the relation Eq. (9) can be modified by assigning the relation Eq. (2) as follows:

$$f_{m,n} = \frac{\pi R f_{0,i} \sqrt{\left(\frac{m}{a}\right)^2 + \left(\frac{n}{b}\right)^2}}{a_{0,i}}.$$ (10)

2. Acoustic element design

2.1 Principle of acoustic element

The acoustic element is based on a rigid frame in the form of a perforated plate or a flexible frame in the form of linear shapes or grids, the back side of which covers a thin carrier layer with a nanofibrous membrane which is covered with frames to some extent against mechanical damage. The frame also has a visual function. The element arrangement based on a perforated panel with a nanofibrous layer wherein the area of the nanofibrous membrane is determined by the size and shape of the perforation which, in general, does not necessarily have to be repeated throughout its shape and size, and the element thus consists of many different sheets that allow vibration of the membrane resulting in the unique properties of each vibrating area. The properties of the cavity resonator also enter the system, where the thickness of the plate and its distance from the reflecting surface (wall/ ceiling application) are also important in addition to the size and spacing of the hole.

The frequency of the perforated panel f_H (Hz), based on the Helmholtz resonator principle, is according to the studies [1, 20] given by an expression:

$$f_H = \frac{c}{2\pi}\sqrt{\frac{S_D}{S_R l d}},$$ (11)

where c (m s^{-1}) is the sound propagation velocity through the medium (air), S_D (m^2) is the cross-sectional area of the cavity, S_R (m^2) is the area of the resonator (hole spacing), l (m) is the thickness of the perforated plate, and d (m) is the distance from the reflective wall.

Figure 1 illustrates an arrangement of a frame-based element in the form of linear structures (wire construction) overlapping the nanofibrous membrane over its entire back surface. Each shape of the frame borders the area of the oscillating
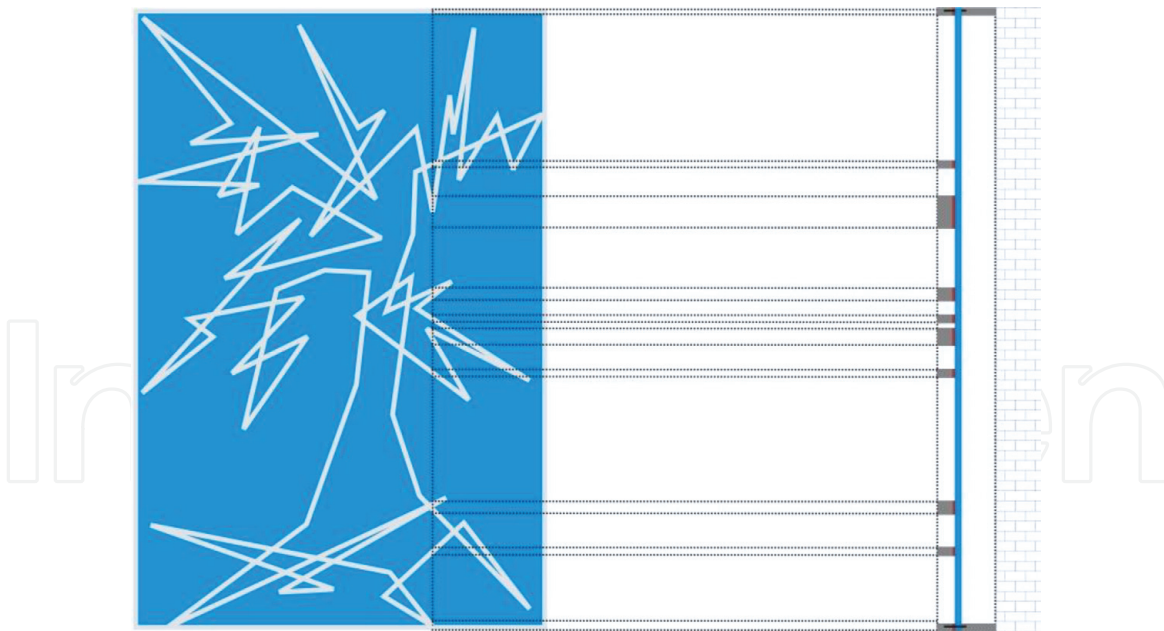
Figure 1.
The principle of designing the final solution of a frame-based acoustic element in the form of linear formations with a nanofibrous layer in view and cut. The gray color in cross section shows the frame (wire construction), the blue one is nanofibrous resonant membrane, and the red one is adhesive.

membrane, and, in general, the individual frame structure does not need to be repeated over the whole surface, and the element thus consists of many different borders that allow vibration of the membrane resulting in the unique properties of each oscillating surface.

2.2 Technical solution

The acoustic element in this case is placed onto a frame—in the form of a regular grid of glass tapes of a negligible thickness—the back side which is covered by a thin carrier layer with a nanofibrous membrane. The design is based on the solution of a general element, placed onto a frame in the form of linear structures with a nanofibrous layer (**Figure 1**), where the grid provides regular open areas with a given size and shape of the holes and their spacing. **Figure 2** compares the sound absorbing properties of an acoustic element with and without a nanofibrous membrane. The proposed element is then compared with commonly used absorbent material with the best sound absorption results that have been measured (**Figure 3**). From this comparison, it is clear that the developed acoustic element can compete with the material that is available on the market with the best results, even at a lower composite element thickness (also assumed with a possible air gap). Compared nanofibrous composite thicknesses are 30, 40, 50, and 60 mm of foam material. The benefits of the proposed technology are the space between the acoustic element of thickness 1–5 mm and the wall/ceiling, which can be used to install lighting, speakers, etc.

2.3 Experimental

2.3.1 Grid design

The basis for the production of a mesh with different mesh size was the R117 A01 structural reinforcing fabric, manufactured by Saint-Gobain Adfors and
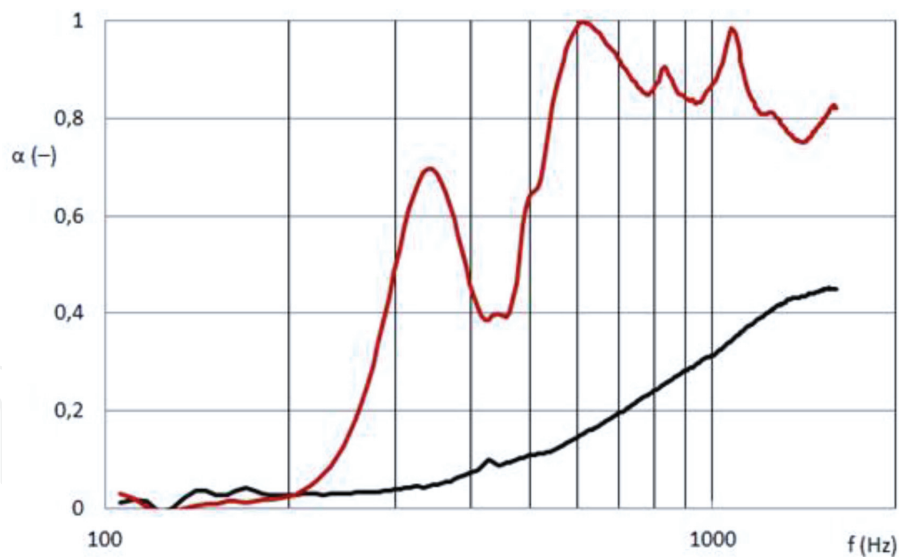
Figure 2.
Frequency dependence of the sound absorption coefficient; comparison of nanofibrous membrane of 0.2 gsm on a carrier of 25 gsm covering the grid of 4 × 4.5 mm mesh size with a thickness of 1 mm with 50 mm air gap (red) and single carrier of 25 gsm covering the same grid of 4 × 4.5 mm mesh size with a thickness of 1 mm with 50 mm air gap (black). Took from [21].
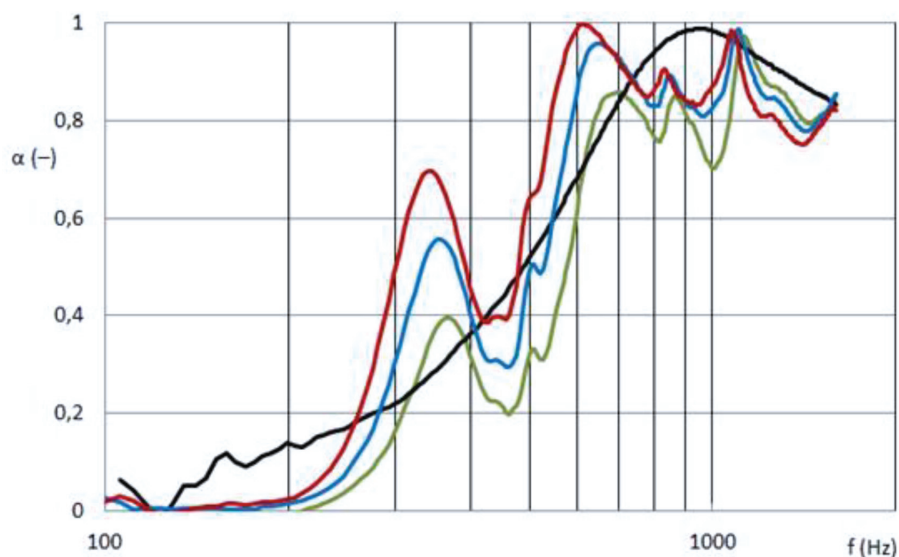

Figure 3.
Frequency dependence of the sound absorption coefficient; comparison of nanofibrous membrane of 0.2 gsm on a carrier of 25 gsm covering the grid of 4 × 4.5 mm mesh size with a thickness of 1 mm with different air gaps (30 mm, green; 40 mm, blue; 50 mm, red) and FOAM 60—foam rectangles with a thickness of 60 mm; width of the base of the rectangle 50 mm foot of the rectangle 40 mm, and top rectangle 60 mm (black). Took from [21].

designed for acrylic plasters. This white grid fabric has a basis weight of 145 g m^{-2} according to the producer, and the mesh spacing has a nominal size of 4.5 × 3.5 mm and a thickness of 0.47 mm.

The smallest mesh size was given by the original dimensions of the grid. The smallest mesh size was determined at 4.1 × 4.3 mm (±0.11 × 0.09 mm) and denoted 1G. The nearest bigger mesh denoted 2G was formed by cutting the weft yarn between two basic meshes at 9.4 × 4.1 mm (±0.11 × 0.11 mm). Another bigger mesh denoted 3G was created by cutting the weft and warp threads between the four basic meshes at 9.0 × 9.4 mm (±0.12 × 0.11 mm). The largest mesh denoted 4G was then formed by cutting out two weft and one warp yarn between the six basic meshes to a size of 9.0 × 14.2 mm (± 0.12 × 0.05 mm) (see **Figure 4**).
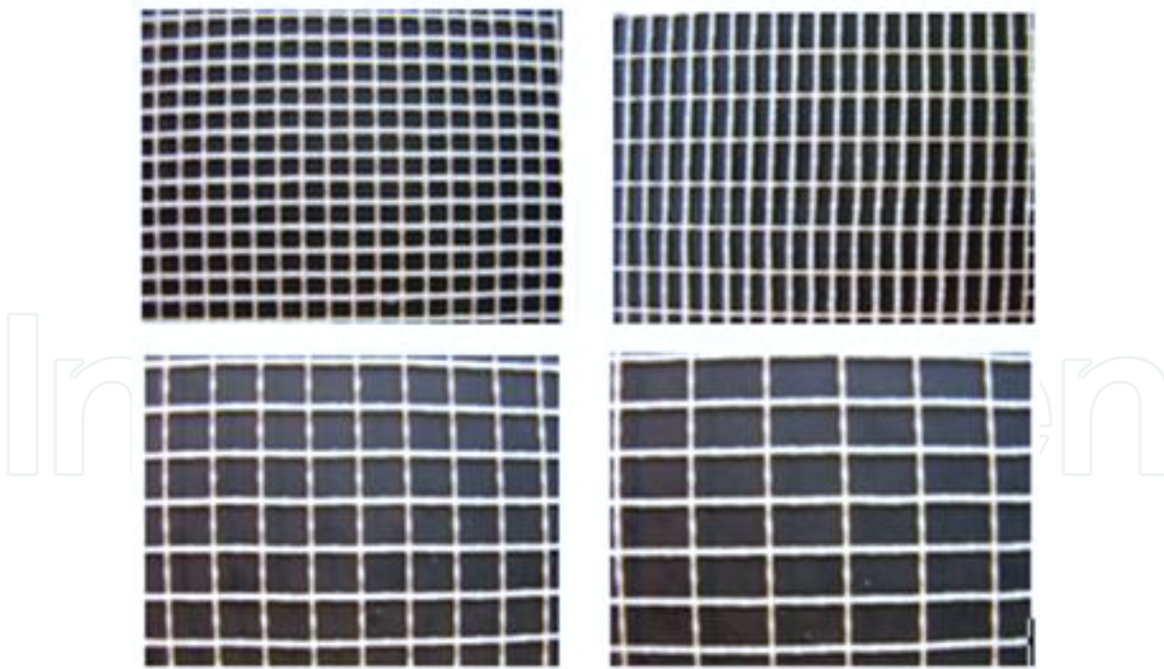
Figure 4.
Photo of applied grids. Rectangle with different side dimensions: 4.1 × 4.3 mm; 9.4 × 4.1 mm; 9.0 × 9.4 mm; 9.0 × 14.2 mm.

2.3.2 Nanofibrous membrane spinning

A nanofibrous layer formed by electrostatic spinning of the polymer from a solution of a 16% polyvinyl alcohol with 40% glyoxal, 85% phosphoric acid, and distilled water was used to produce the membrane. For production of PA6 nanofibrous membrane, a needleless electrospinning method from a cord was employed (Nanospider^{TM}, NS 1WS500U). In this method [22], there is a solution carriage-feeding liquid polymeric material around a moving stainless steel wire. The wire electrode is connected to high-voltage supplier, and on the top, there is a grounded counter electrode. When the applied voltage exceeds a critical value, Taylor cones are then created on the wire surface, oriented toward the counter electrode. PA6 solution jets move toward the collector, and as the solvent evaporates, the PA6 nanofibrous layer is collected on a moving substrate.

The basis weight of the nanofibrous layer is given by the takeoff speed of the backing strip in the electrostatic spinning process. Four basis weights of the nanofibrous layer, namely, 6 g m^{-2} (exact value 5.7 ± 0.2 g m^{-2}), were formed at a corresponding process rate of 0.04 m min^{-1}, 3 g m^{-2} (exact value 2.6 ± 0.15 g m^{-2}) at a corresponding process rate of 0.09 m min^{-1}, 2 g m^{-2} (exact value 2.2 ± 0.03 g m^{-2}) at a corresponding process rate of 0.14 m min^{-1}, and 1 g m^{-2} (exact value 1.7 ± 0.01 g m^{-2}) at a corresponding process rate of 0.18 m min^{-1}. During the spinning on the Nanospider laboratory, a constant temperature of 22.4° C and a relative humidity of 44% RH were maintained with the built-in air conditioner. The spinning process was 0.33–0.34 mA and 50 kV. The distance of electrodes was 150 mm. In **Figures 5** and **6**, the thickness of nanofiber layer of different basis weights was determined using scanning electron microscopy (SEM). A small section of the fiber mat was placed on the SEM sample holder and sputter coated with gold (Quorum Q150R rotary-pumped sputter coater). Carl Zeiss Ultra Plus Field Emission SEM using an accelerating voltage of 1.48 kV was employed to take the SEM photographs.
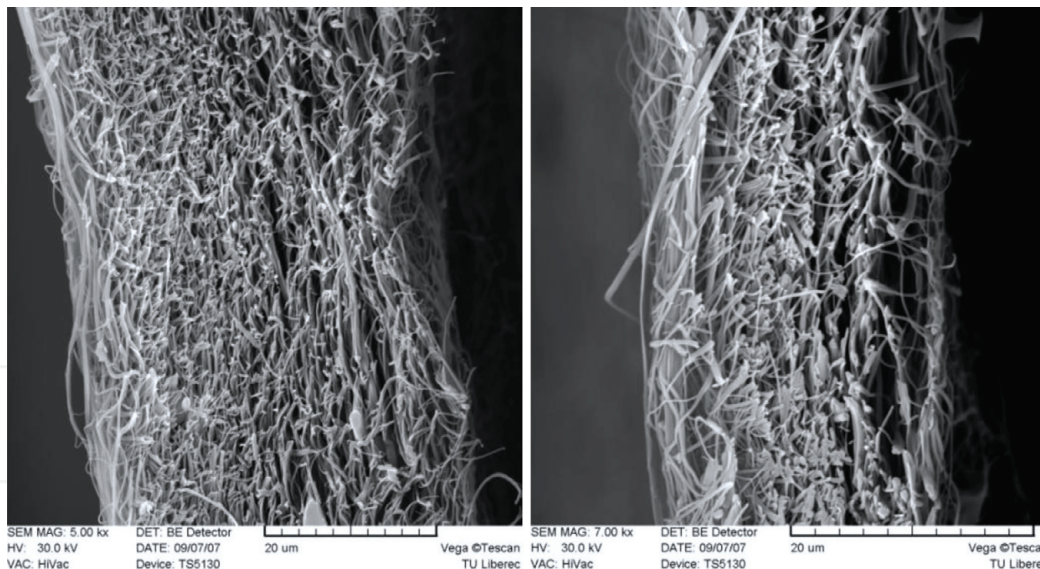
Figure 5.
SEM images of PVA nanofibers of basis weights 6 (5.7 ± 0.2) g m⁻² (on the left) and 3 (2.6 ± 0.15) g m⁻² (on the right).
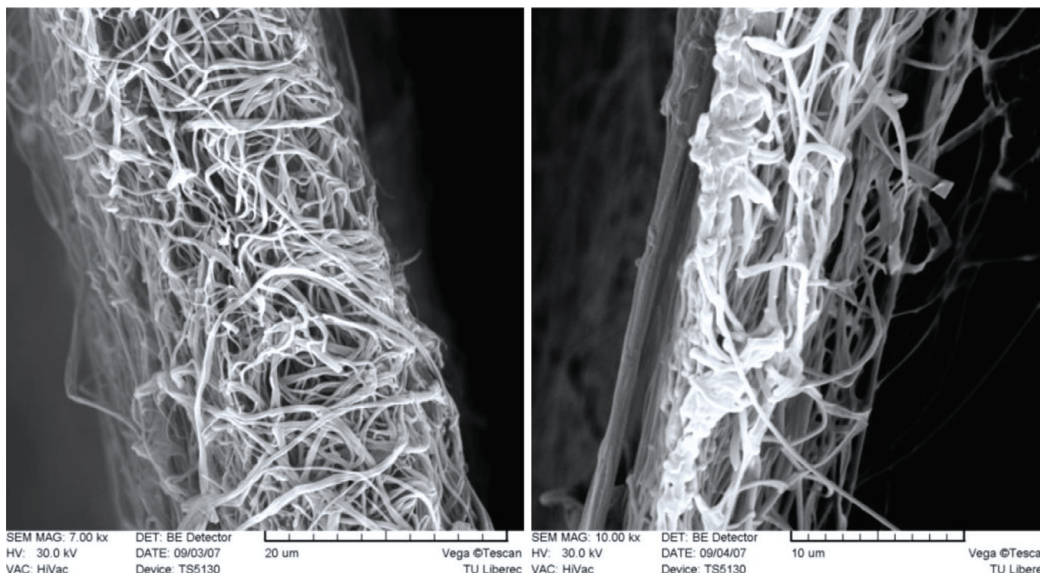

Figure 6.
SEM images of PVA nanofibers of basis weights 2 (2.2 ± 0.03) g m⁻² (on the left) and 1 (1.7 ± 0.01) g m⁻² (on the right).

2.3.3 Sound absorption measurement

Two-microphone impedance measurement tube typ. 4206 was used to measure the absorption coefficient in the frequency ranges 50 Hz to 6.4 kHz (standard large tube setup for samples diameter 100 mm: 50 Hz to 16 kHz; standard small tube setup for samples diameter 29 mm: 500 Hz to 6.4 kHz). The test was made according to standard ISO 10534-2. The analyzer (Aubion X.8) generates a random signal which is then amplified by a power amplifier (B&K Typ. 2670, Crown D-75A); frequency is weighted by the frequency weighting unit in the large tube and then applied to the loudspeaker. The analyzer finally measures the response of the two microphones (B&K Typ. 4187) and calculates the frequency response function between these two microphone channels, so the data can be obtained from

it. The amount of sound energy which is absorbed is described as the ratio of sound energy absorbed to the sound energy incident and is termed the sound absorption coefficient α. The average of the five measurements was shown. The nanofiber layer was set at a distance of 30 mm from the reflective wall so that the nanofibrous membrane was able to vibrate under the incident sound wave as it is demonstrated on **Figure** 7.

2.3.4 Optical method for determination of resonant frequency

The optical method for determining the resonance frequencies of the membranes [19] was used to calculate the velocity of transverse wave on the homogeneous circular membrane C_M. The main components of the system were the digital camera (Olympus—System i-SPEED2), a LCD display panel of 8.4″, and a transparent tube (see **Figure 8**). The test sample was fixed inside the tube. The incident plane sinusoidal sound wave was excited by a speaker located at end of the tube. The membrane began to oscillate after the impact sound waves reached, and its movement was picked by the high-speed digital camera and in turn was displayed on the LCD.

In order to determine the resonant frequency of the membrane, the 1-1500 Hz frequency range was studied by taking measurements at every 20 Hz to obtain a rough estimate of the resonant frequency. The deflection size of the nanofibrous membrane under the frequency range of 1–1500 Hz was measured using the closed tube. The resonant frequencies of the circular membrane of radius 0.05 m and 1 g m^{-2} basis weight have been detected as can be seen in **Table 1**. The velocity of transverse wave on the homogeneous circular membrane C_M has been determined by the relationship Eq. (2) based on the measured first resonant frequency $f_{0,1}$ equal to 90 Hz.
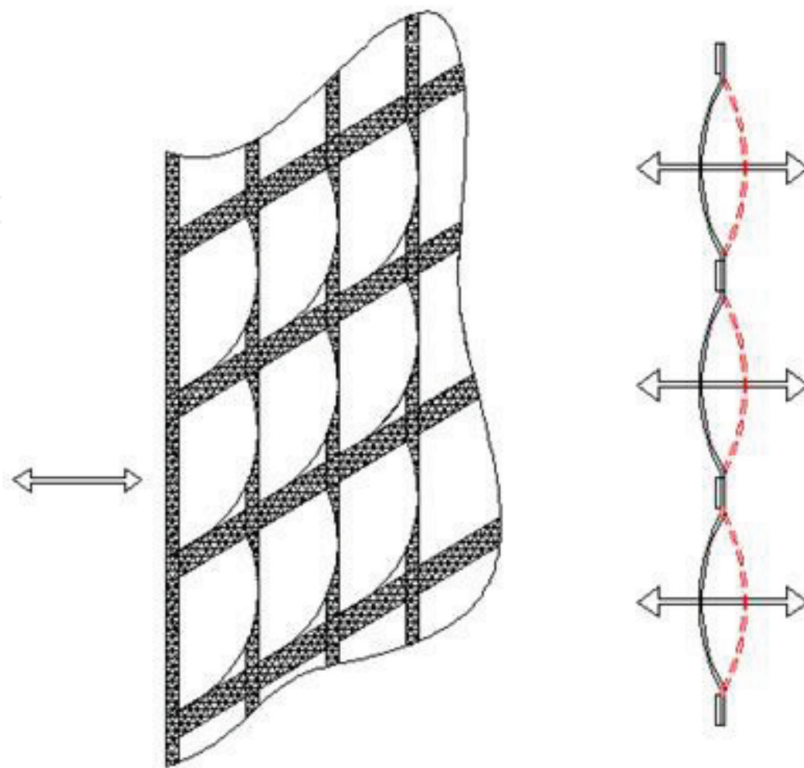

Figure 7.
Illustration of the deflection of vibrating membrane inside the meshes of a grid.

Figure 8.
Scheme of the measuring system. Took from [19].

Circular membrane		$f_{0,i}$ (Hz)	R (m)	C_M (m s^{-1})
$a_{0,1}$	2.4048	90	0.05	11.76
$a_{0,2}$	5 5201	207	0.05	11.76
$a_{0,3}$	8 6537	324	0.05	11.76
$a_{0,4}$	11 7915	441	0.05	11.76

Table 1.
Calculation of the velocity of transverse wave on the membrane C_M based on measured resonant frequency of vibrating circular membrane of radius 0.05 m and 1 g m^{-2} basis weight (a).

3. Sound absorption results

In this arrangement, the idea is connecting the membrane (nanofibrous) resonator together with the mesh frame. The resonant frequencies $f_{m,n}$ of rectangle membrane with a variation of the side dimension are determined according to formula Eq. (10). The calculated resonant frequencies relating to vids m and n are shown in **Tables 2–5**. The dependence of the measured sound absorption coefficient on the sound frequency is shown in the following **Figures 9–16**. In **Figures 9–12**, the measured frequency dependence of the sound absorption coefficient for samples of the same basis weight and different mesh size is compared.

From the curves on **Figures 9–12** describing the frequency dependence of the sound absorption coefficient for samples of the same basis weight and different mesh size, it can be seen that the two clear sound absorption peaks occur in the case of small mesh size (1G and 2G), while in the case of large meshes (3G and 4G), only one clear sound absorption peak exists. It can be seen, therefore, that the mesh size of the grid has a major impact on the amount of the sound absorption coefficient. It can also be observed from **Figure 9** that the nanofibrous membrane of highest basis weight (6 g m^{-2}) applied on the smaller meshes is better at dampening frequencies in the range of approximately 1500 Hz and 4000–5000 Hz, while the nanofiber layer deposited on the larger meshes is better at dampening frequencies of 2500–3000 Hz. Appearance of the peak for the smaller mesh (1G, 2G) at similar frequencies can be explained by the fact that the both meshes have the same width

1G Mesh size 4.1;4.3				a (m)	b (m)	C_M (m s^{-1})	$f_{m,n}$ (Hz)
m	1	n	1	0.0041	0.0043	11.76	1981
m	1	n	2	0.0041	0.0043	11.76	3087
m	2	n	1	0.0041	0.0043	11.76	3177
m	2	n	2	0.0041	0.0043	11.76	3962
m	3	n	1	0.0041	0.0043	11.76	4514
m	3	n	2	0.0041	0.0043	11.76	5097
m	3	n	3	0.0041	0.0043	11.76	5943
m	1	n	3	0.0041	0.0043	11.76	4345
m	2	n	3	0.0041	0.0043	11.76	5005

Table 2.
Calculation of resonant frequencies of a rectangle membrane with 1 g m^{-2} basis weight of 4.1 × 4.3 mm side dimension; the vids m and n and rectangle dimensions a and b are mentioned.

2G Mesh size 9.4;4.1				a (m)	b (m)	C_M (m s^{-1})	$f_{m,n}$ (Hz)
m	1	n	1	0.0094	0.0041	11.76	1564
m	1	n	2	0.0094	0.0041	11.76	2935
m	2	n	1	0.0094	0.0041	11.76	1903
m	2	n	2	0.0094	0.0041	11.76	3129
m	3	n	1	0.0094	0.0041	11.76	2361
m	3	n	2	0.0094	0.0041	11.76	3427
m	3	n	3	0.0094	0.0041	11.76	4693
m	1	n	3	0.0094	0.0041	11.76	4347
m	2	n	3	0.0094	0.0041	11.76	4480

Table 3.
Calculation of resonant frequencies of a rectangle membrane with 1 g m^{-2} basis weight of 9.4 × 4.1 mm side dimension; the vids m and n and rectangle dimensions a and b are mentioned.

3G Mesh size 9.0; 9.4				a (m)	b (m)	C_M (m s^{-1})	$f_{m,n}$ (Hz)
m	1	n	1	0.009	0.0094	11.76	904
m	1	n	2	0.009	0.0094	11.76	1411
m	2	n	1	0.009	0.0094	11.76	1448
m	2	n	2	0.009	0.0094	11.76	1809
m	3	n	1	0.009	0.0094	11.76	2057
m	3	n	2	0.009	0.0094	11.76	2325
m	3	n	3	0.009	0.0094	11.76	2713
m	1	n	3	0.009	0.0094	11.76	1987
m	2	n	3	0.009	0.0094	11.76	2286

Table 4.
Calculation of resonant frequencies of a rectangle membrane with 1 g m^{-2} basis weight of 9.0 × 9.4 mm side dimension; the vids m and n and rectangle dimensions a and b are mentioned.

| 4G Mesh size 9.0;14.2				a (m)	b (m)	C_M (m s^{-1})	$f_{m,n}$ (Hz)
m	1	n	1	0.009	0.0142	11.76	773
m	1	n	2	0.009	0.0142	11.76	1055
m	2	n	1	0.009	0.0142	11.76	1370
m	2	n	2	0.009	0.0142	11.76	1547
m	3	n	1	0.009	0.0142	11.76	2003
m	3	n	2	0.009	0.0142	11.76	2127
m	3	n	3	0.009	0.0142	11.76	2320
m	1	n	3	0.009	0.0142	11.76	1403
m	2	n	3	0.009	0.0142	11.76	1803

Table 5.
Calculation of resonant frequencies of a rectangle membrane with 1 g m^{-2} basis weight of 9.0 × 14.2 mm side dimension; the vids m and n and rectangle dimensions a and b are mentioned.
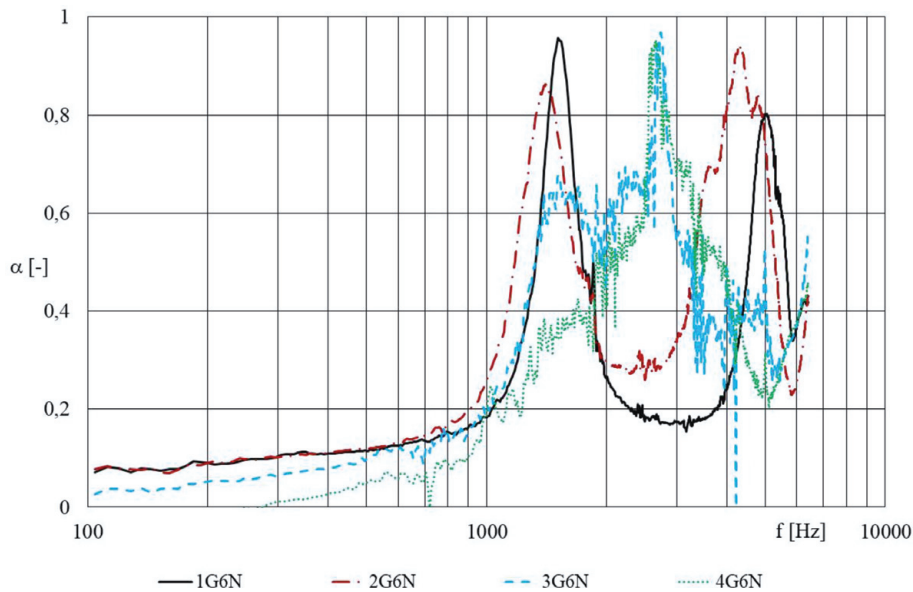
Figure 9.
Frequency dependence of the sound absorption coefficient; comparison of nanofibrous membrane of 6 g m^{-2} covering the grid of different mesh sizes: 1G_4.1 × 4.3 mm; 2G_9.4 × 4.1 mm; 3G_9.0 × 9.4 mm; 4G_9.0 × 14.2 mm. The air gap between the sample of 1 mm thickness and reflective wall was 30 mm.

of 4.1 mm, which is provides the same deviation in the one of axis, regardless of the total area of the mesh. The similar phenomenon can be seen for the highest meshes (3G and 4G) where the constant dimension of meshes is 9 mm with result of identical one of sound absorption peaks for all sample configurations (**Figures 9–12**).

Subsequently, the influence of the basis weight of the nanolayer spun on a grid of the same mesh size onto the maximum values of the sound absorption coefficient in relation to the frequency was examined (see **Figures 13–16**). By checking the grids themselves (gray curve on **Figures 13–16**), almost identical curves of all mesh sizes were found, with only the minimum values of the sound absorption coefficient. It can be said, therefore, that the mass of the carrier grid alone does not significantly influence the course of the sound absorption curves. The basis weight influence on the sound absorption is given by the theory Eqs. (2) and (3) where the resonant frequency of homogenous membrane decreases with its increasing basis weight. The
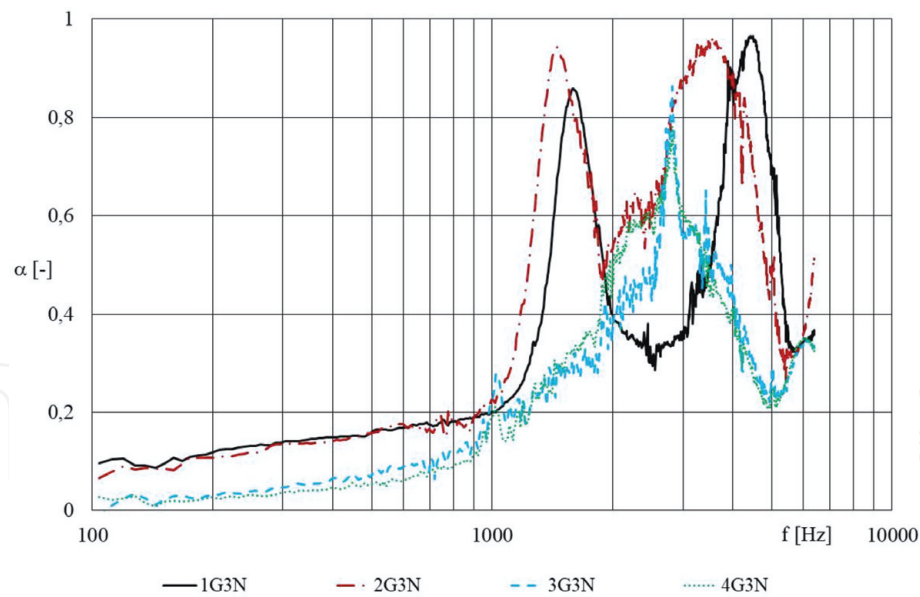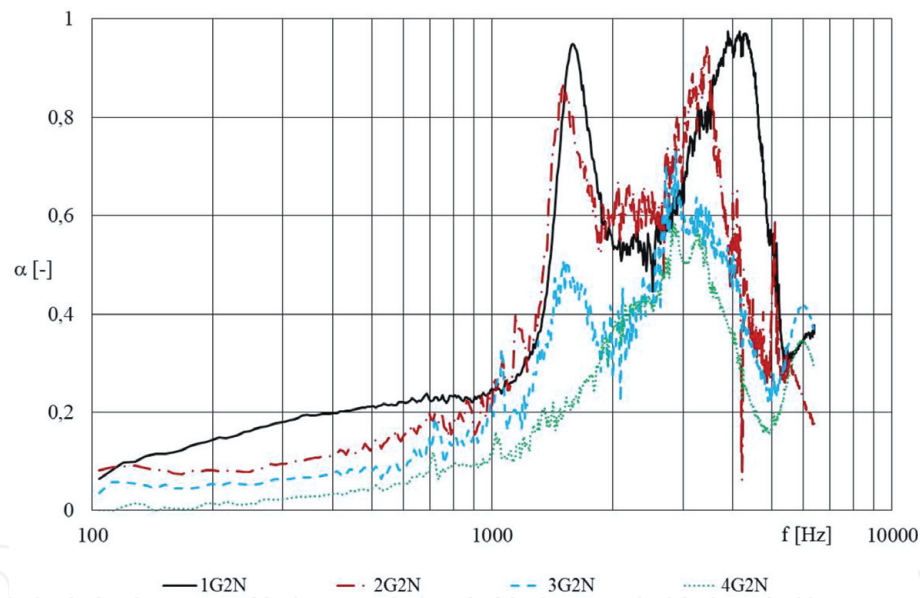
Figure 10.
Frequency dependence of the sound absorption coefficient; comparison of nanofibrous membrane of 3 g m⁻²
covering the grid of different mesh sizes: 1G_4.1 × 4.3 mm; 2G_9.4 × 4.1 mm; 3G_9.0 × 9.4 mm;
4G_9.0 × 14.2 mm. The air gap between the sample of 1 mm thickness and reflective wall was 30 mm.

Figure 11.
Frequency dependence of the sound absorption coefficient; comparison of nanofibrous membrane of 2 g m⁻²
covering the grid of different mesh sizes: 1G_4.1 × 4.3 mm; 2G_9.4 × 4.1 mm; 3G_9.0 × 9.4 mm;
4G_9.0 × 14.2 mm. The air gap between the sample of 1 mm thickness and reflective wall was 30 mm.

influence of basis weight on the sound absorption coefficient is not clear for these measured configurations. For the smaller meshes (1G and 2G), the sound absorption increases with decreasing basis weight of nanofibrous membrane. Then the antiresonance effect of heavy membrane where the acoustic element loses sound absorption ability (approx. 2500 Hz) occurs due to undamped vibrating membrane. For the higher meshes, the antiresonance effect does not occur because of the grid configuration with the 30 mm air gap does not allow sound absorption below 1500 Hz where the first resonant frequency should cause the first sound absorption peak.

The resonant frequencies with relevant sound absorption coefficients are summarized in **Table 6**. The resonant frequency for membrane of 1 g m⁻² (lightest
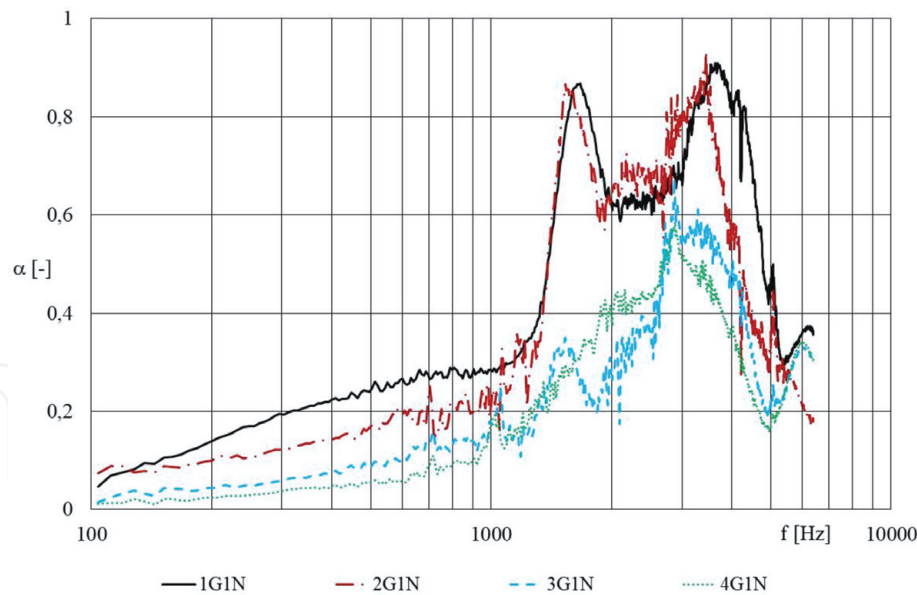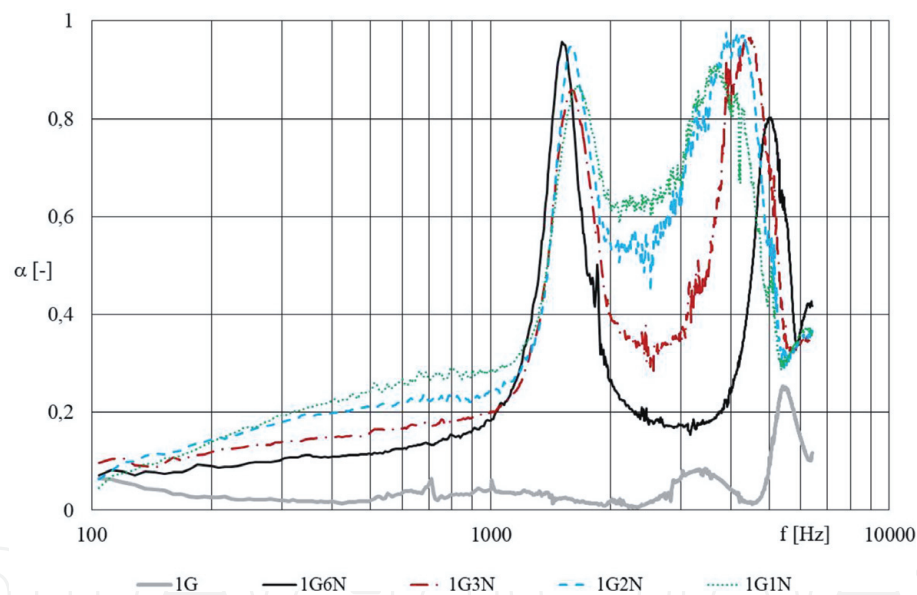
Figure 12.
Frequency dependence of the sound absorption coefficient; comparison of nanofibrous membrane of 1 g m^{-2} covering the grid of different mesh sizes: 1G_4.1 × 4.3 mm; 2G_9.4 × 4.1 mm; 3G_9.0 × 9.4 mm; 4G_9.0 × 14.2 mm. The air gap between the sample of 1 mm thickness and reflective wall was 30 mm.

Figure 13.
Frequency dependence of the sound absorption coefficient; comparison of nanofibrous membrane of different basis weights (6N_6 g m^{-2}; 3 N_3 g m^{-2}; 2 N_2 g m^{-2}; 1 N_1 g m^{-2}) covering the grid of mesh size 4 1 × 4.3 mm. 2G_9.4 × 4.1 mm; 3G_9.0 × 9.4 mm; 4G_9.0 × 14.2 mm. The air gap between the sample of 1 mm thickness and reflective wall was 30 mm.

column on the right) can be compared with the calculated values from **Tables 2–5**. The measured values of resonant frequency are in a good agreement for samples with mesh grid 1G where the calculated value of the first and second resonant frequency $f_{1,1}$ = 1981 Hz and $f_{2,2}$ = 3962 Hz (**Table 2**) can be compared with the measured first and second resonant frequencies f_1 = 1672 Hz and f_1 = 3696 Hz (**Table 6**) given by the sound absorption peaks from **Figure 12**. Analogous to the results, the samples with mesh grid 2G where the calculated value of the first and second resonant frequencies $f_{1,1}$ = 1564 Hz and $f_{2,2}$ = 3129 Hz (**Table 2**) can be compared with the measured first and second resonant frequencies f_1 = 1536 Hz and
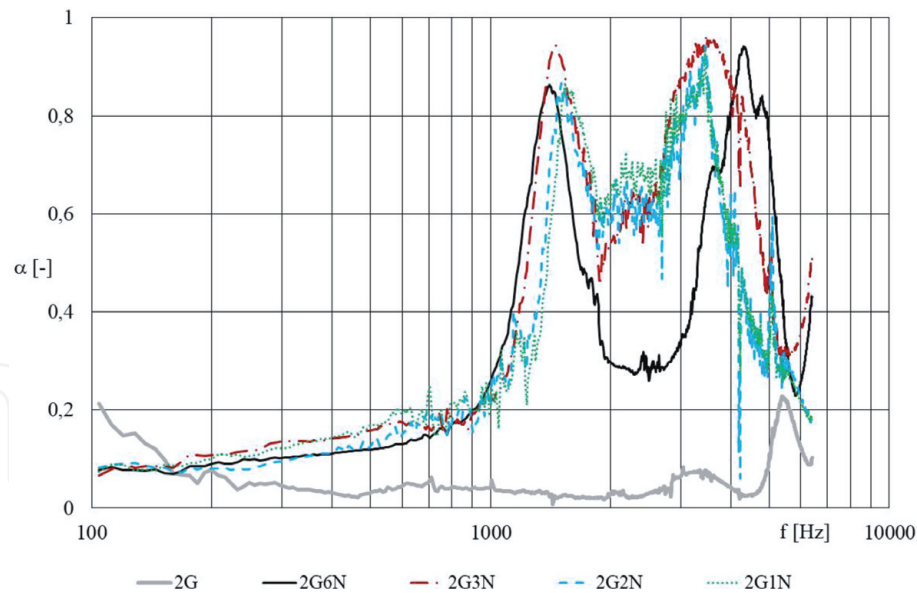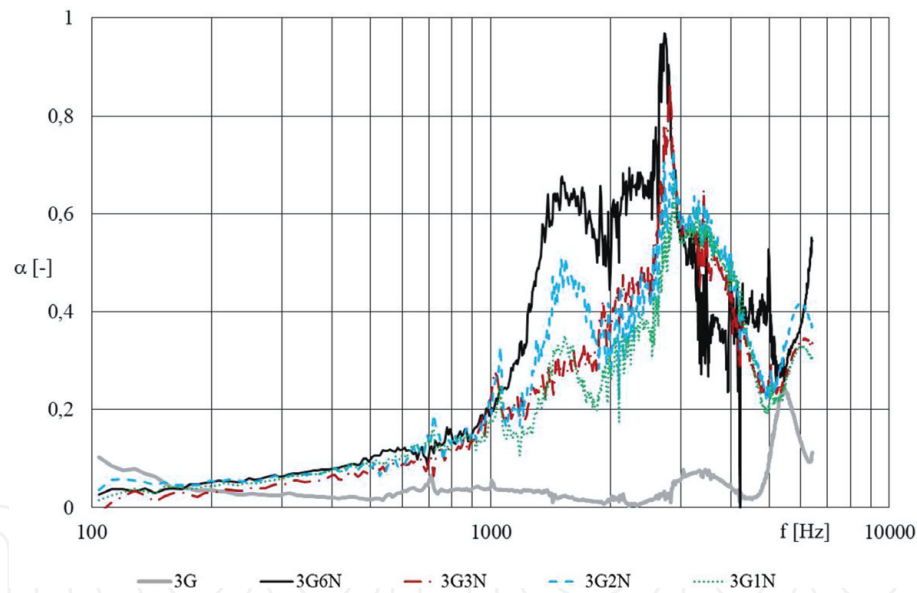
Figure 14.
Frequency dependence of the sound absorption coefficient; comparison of nanofibrous membrane of different basis weights (6N_6 g m^{-2}; 3 N_3 g m^{-2}; 2 N_2 g m^{-2}; 1 N_1 g m^{-2}) covering the grid of mesh size 9.4 × 4.1 mm. The air gap between the sample of 1 mm thickness and reflective wall was 30 mm.

Figure 15.
Frequency dependence of the sound absorption coefficient; comparison of nanofibrous membrane of different basis weights (6N_6 g m^{-2}; 3 N_3 g m^{-2}; 2 N_2 g m^{-2}; 1 N_1 g m^{-2}) covering the grid of mesh size 9.0 × 9.4 mm. The air gap between the sample of 1 mm thickness and reflective wall was 30 mm.

f_1 = 3448 Hz (**Table 6**) given by the sound absorption peaks from **Figure 12**. The samples with mesh grid 3G where the calculated value of first and second resonant frequency $f_{1,1}$ = 904 Hz and $f_{2,2}$ = 1809 Hz (**Table 2**) can be compared with the measured first and second resonant frequencies f_1 = 1056 Hz and f_1 = 1536 Hz (**Table 6**) given by the sound absorption peaks from **Figure 12**. The clear sound absorption peaks of sample with mesh grid 4G do not occur. That is why the comparison cannot be done.
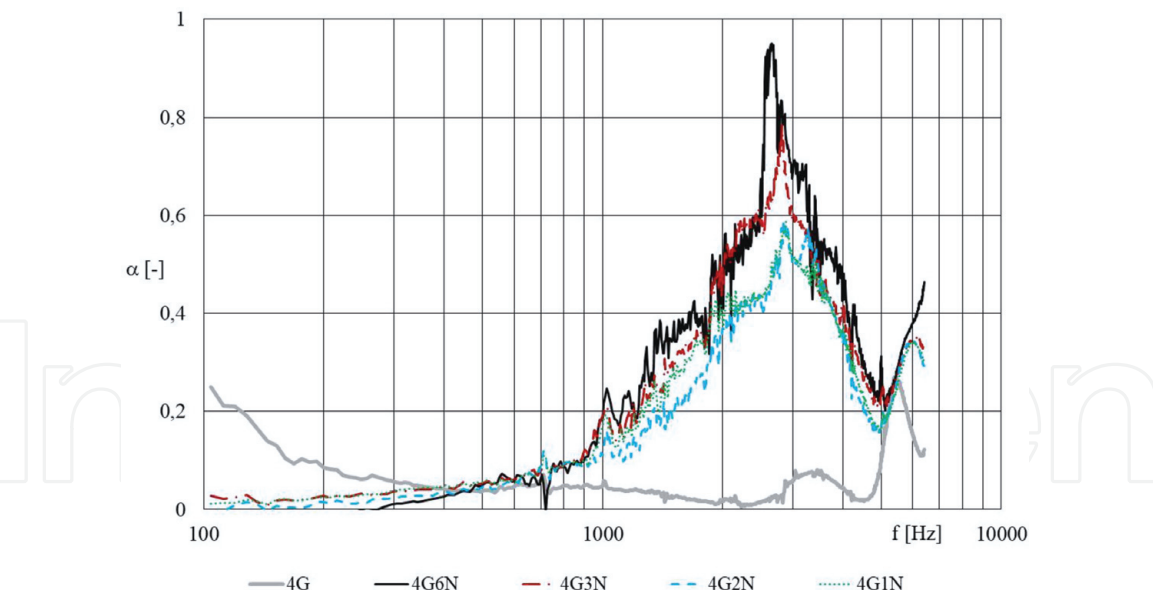
Figure 16.
Frequency dependence of the sound absorption coefficient; comparison of nanofibrous membrane of different basis weights ($6N\_6\ g\ m^{-2}$; $3\ N\_3\ g\ m^{-2}$; $2\ N\_2\ g\ m^{-2}$; $1\ N\_1\ g\ m^{-2}$) covering the grid of mesh size 9.0×14.2 mm. The air gap between the sample of 1 mm thickness and reflective wall was 30 mm.

1G mesh with membrane 6 N			1G mesh with membrane 3 N			1G mesh with membrane 2 N			1G mesh with membrane 1 N		
α	f_1 (Hz)	f_2 (Hz)	α	f_1 (Hz)	f_2 (Hz)	α	f_1 (Hz)	f_2 (Hz)	α	f_1 (Hz)	f_2 (Hz)
0.858	1600		0.858	1600		0.95	1592		0.867	1672	
0.801		5008	0.966		4432	0.974		3896	0.906		3696
2G mesh with membrane 6 N			**2G mesh with membrane 3 N**			**2G mesh with membrane 2 N**			**2G mesh with membrane 1 N**		
α	f_1 (Hz)	f_2 (Hz)	α	f_1 (Hz)	f_2 (Hz)	α	f_1 (Hz)	f_2 (Hz)	α	f_1 (Hz)	f_2 (Hz)
0.944	1456		0.943	1456		0.95	1592		0.867	1536	
0.941		4312	0.958		3560	0.943		3448	0.934		3448
3G mesh with membrane 6 N			**3G mesh with membrane 3 N**			**3G mesh with membrane 2 N**			**3G mesh with membrane 1 N**		
α	f_1 (Hz)	f_2 (Hz)	α	f_1 (Hz)	f_2 (Hz)	α	f_1 (Hz)	f_2 (Hz)	α	f_1 (Hz)	f_2 (Hz)
0.677	1512		0.863	2816		0.51	1536		0.25	1056	
0.968		2728	0.651		3424	0.731		2872	0.349		1536
4G mesh with membrane 6 N			**4G mesh with membrane 3 N**			**4G mesh with membrane 2 N**			**4G mesh with membrane 1 N**		
α	f_1 (Hz)	f_2 (Hz)	α	f_1 (Hz)	f_2 (Hz)	α	f_1 (Hz)	f_2 (Hz)	α	f_1 (Hz)	f_2 (Hz)
0.95	2656		0.783	2816		0.586	2840		—	—	
—		—	—		—	0.57		3272	—		—

Table 6.
Measured resonant frequencies of a rectangle membrane of different basis weights and different side dimensions. The sound absorption coefficient α is mentioned for each resonant frequency rectangle membrane.

4. Conclusions

This chapter has studied the behavior of nanofibrous membrane in a synergy with a grid over the sound waves incidence. The sound absorption coefficient of a frame-based element in the form of linear structures overlapping the nanofibrous membrane over its entire back surface has been measured. A nanofibrous membrane having a basis weight of 6, 3, 2, and 1 g m^{-2} covering a rectangle grid with the different side dimensions, 4.1 × 4.3 mm, 9.4 × 4.1 mm, 9.0 × 9.4 mm, and 9.0 × 14.2 mm, has been placed at a constant distance of 30 mm from the reflective wall. Two-microphone impedance measurement tube typ. 4206 was used to measure the absorption coefficient in the frequency ranges 50 Hz to 6.4 kHz according to standard ISO 10534-2.

By measuring the sound absorption of nanofibrous layers with the same area weights covering the grids of different mesh sizes, it was found that the nanofiber layer applied on smaller mesh achieves better sound absorption where two absorption peaks occur at approximately 1500 and 3500 Hz, while nanofibrous membrane applied to the larger mesh grids does not absorb the sound of these frequencies enough. From the analysis of sound absorption measurement results, it can be assumed that the mass of the carrier grid alone does not significantly influence the course of the sound absorption curves. The influence of basis weight on the sound absorption coefficient is not clear for all measured configurations. For the smaller meshes, the sound absorption increases with decreasing basis weight of nanofibrous membrane. Then the antiresonance effect of heavy membrane where the acoustic element loses sound absorption ability (approx. 2500 Hz) occurs due to undamped vibrating membrane. The maximum values of the sound absorption coefficient occur at resonant frequencies of the sound absorption system. The resonant frequencies of 1 g m^{-2} membrane have been compared with the calculated values, whereas the calculated and measured values are in a good agreement.

Conflict of interest

The author(s) declared no potential conflicts of interest with respect to the research, authorship, and/or publication of this article.

Author details

Klara Kalinova
Technical University of Liberec, Liberec, Czech Republic

*Address all correspondence to: klara.kalinova@tul.cz

IntechOpen

References

[1] Kolmer F, Kyncl J. Prostorová akustika. 1st ed. Prague: SNTL; 1980. ISBN 04-514-80

[2] Coates M, Kierzkowski M. Acoustic textiles - lighter, thinner and more sound-absorbent. Technical Textiles International. 2002;**11**(7):15-18

[3] Sakagami K et al. Detailed analysis of the acoustic properties of a permeable membrane. Applied Acoustics. 1998; **54**(2):93-111

[4] Takahashi D, Sakagami K, Morimoto M. Acoustic properties of permeable membranes. The Journal of the Acoustical Society of America. 1996;**99**: 3003-3009

[5] Sakagami K et al. Sound absorption of a cavity-backed membrane : A step towards design method for membrane-type absorbers. Applied Acoustics. 1996; **49**(3):237-247

[6] Sakagami K et al. Acoustic properties of an infinite elastic plate with a back cavity. Acustica. 1993;**78**:288-295

[7] Kiyama M et al. A basic study on acoustic properties of double-leaf membranes. Applied Acoustics. 1998; **54**(3):239-254

[8] Sakagami K, Kiyama M, Morimoto M. Acoustic properties of double-leaf membranes with a permeable leaf on sound incidence side. Applied Acoustics. 2002;**63**(8):911-926

[9] Kang J, Fuchs HV. Predicting the absorption of open weave textiles and micro-perforated membranes backed by an air space. Journal of Sound and Vibration. 1999;**220**(5):905-920

[10] Ackermann U, Fuchs HV, Rambausek N. Sound absorbers of a novel membrane construction. Applied Acoustics. 1988;**25**(3):197-215

[11] Wang CY. Some exact solution of the vibration of non-homogenous membranes. Journal of Sound and Vibration. 1998;**210**(4):555-558

[12] Gottlieb HPW. Exact solutions for vibrations of some annular membranes with inhomogeneous radial densities. Journal of Sound and Vibration. 2000; **233**(1):165-170

[13] Jabareen M, Eisenberger M. Free vibrations of non-homogenous cirkular and annular membranes. Journal of Sound and Vibration. 2001;**240**(3): 409-429

[14] Wang CY. Vibration of an annular membrane attached to a free rigid core. Journal of Sound and Vibration. 2003; **260**(4):776-782

[15] Pinto F. Analytical and experimental investigation on a vibrating annular membrane attached to a central free, rigid core. Journal of Sound and Vibration. 2006;**291**(3):1278-1287

[16] Wang CY. Fundamental models of a cirkular membrane with radial constraints on the boundary. Journal of Sound and Vibration. 1999;**220**(3): 559-563

[17] Kwak MK. Vibration of circular membranes in contact with water. Journal of Sound and Vibration. 1994; **178**(5):688-690

[18] Škvor Z. Akustika a elektroakustika. 1st ed. Academia Praha: Prague; 2001. ISBN 80-200-0461-0

[19] Kalinova K, Ozturk MK, Komarek M. Open and closed tube method for determination of resonance frequencies of nanofibrous membrane. The Journal

of The Textile Institute. 2016;**107**(8): 1068-1078. DOI: 10.1080/ 00405000.2015.1083353

[20] Randeberg RT. Perforated panel absorbers with viscous energy dissipation enhanced by orifice design. PhD [thesis], 1st edition. Trondheim: NTNU; 2000. Available from: https://b rage.bibsys.no/xmlui/bitstream/handle/ 11250/249798/125365_FULLTEXT01. pdf?sequence=1&isAllowed=y

[21] Kalinova K. A sound absorptive element comprising an acoustic resonance Nanofibrous membrane. Recent Patents on Nanotechnology. 2015;**9**(1):61-69. ISSN 1872-2105

[22] Jirsak O, SanetrnikF, et al. Method of nanofibres production from a polymer solution using electrostatic spinning and a device for carrying out the method. Patent WO2005024101 (US2006290031); 2005